Available online at www.sciencedirect.com
SCIENCE DIRECT®
Cement & Concrete Composites 28 (2006) 173–188
Cement & Concrete Composites
www.elsevier.com/locate/cemconcomp

Damaging effects of deicing chemicals on concrete materials

Kejin Wang [a,*], Daniel E. Nelsen [a], Wilfrid A. Nixon [b]

[a] Iowa State University, 492 Town Engineering, Ames, IA 50011, USA
[b] University of Iowa, 4121 Seamans Center, Iowa City, IA 52242, USA

Received 17 March 2005; accepted 21 July 2005
Available online 2 November 2005

Abstract

The damaging impact of various deicing chemicals and exposure conditions on concrete materials was investigated. Five deicing chemicals (sodium chloride, calcium chloride with and without a corrosion inhibitor, potassium acetate, and an agricultural product) were studied. Freezing–thawing (F–T) and wetting–drying (W–D) exposure conditions were considered. Mass loss, scaling, compressive strength, chemical penetration, and micro-structure of the paste and concrete subjected to these deicing chemicals and exposure conditions were evaluated. Results indicated that the various deicing chemicals penetrated at different rates into a given paste and concrete, resulting in different degrees of damage. Among the deicing chemicals tested, two calcium chloride solutions caused the most damage. Addition of a corrosion inhibitor into the calcium chloride solution delayed the onset of damage, but it did not reduce the ultimate damage. Chloride-related deicing chemicals often brought about leaching of calcium hydroxide, as well as chemical alterations in concrete. Potassium acetate caused minor scaling, associated with alkali carbonation of the surface layer of concrete. Although producing a considerable number of micro-pores on the surface of the samples, the agricultural deicing product resulted in the least chemical penetration and scaling damage of paste and concrete.

Keywords: Deicing; Wetting–drying; Freezing–thawing; Mass loss; Scaling; Strength

1. Introduction

Deicing chemicals often exacerbate concrete damage originating from freezing and thawing (F–T). Besides creating pressures through osmosis and crystallization, deicing chemicals generally increase the degree of concrete saturation and keep concrete pores at or near maximum fluid saturation, thus increasing the risk of frost damage [1]. The salts in deicing solutions also decrease the freezing point of concrete pore solution, leading to significant hydraulic pressure [2]. Because the salt concentration varies with the distance from the exposed concrete surfaces, various amount of ice may form in different layers under the concrete surface, resulting in deformation of the layers and generation of pressure between the layers. Freezing of an upper layer (such as the surface layer, which often occurs at a low deicing chemical concentration) may prohibit escape of the supercooled liquids from the internal layers, thus developing considerable hydraulic pressure. Therefore, the combined effect of the hydraulic, osmotic and crystallization pressures below the surface lead to scaling of the concrete [3].

Aggravated damage may also be attributed to chemical interactions between deicing chemicals and concrete materials. Chemical deterioration of the concrete may result from leaching and decomposition of cement hydration products [4–6], as well as accelerated concrete carbonation [7] and alkali–silica reaction (ASR) [8,9]. Research has demonstrated that salt substitutes or deicing salts with a corrosion inhibitor also interact with concrete materials and lead to precipitate production [4,10]. It is believed that concrete deterioration due to deicing chemicals may begin with physical reactions, which generate micro- and macro-cracks in concrete. Because the cracks make concrete more permeable and more vulnerable to the ingress of deicing

* Corresponding author. Tel.: +1 515 294 2152; fax: +1 515 294 8216.
E-mail address: kejinw@iastate.edu (K. Wang).

0958-9465/$ - see front matter © 2005 Elsevier Ltd. All rights reserved.
doi:10.1016/j.cemconcomp.2005.07.006

chemical ions, chemical deterioration is then provoked [11]. Generally, the combined effect of physical and chemical deterioration is more severe than that from the simple sum of individual reaction.

Despite an ongoing awareness on deicing chemical damage to concrete, the relative degree of damage from different deicing chemicals under different environmental conditions is not thoroughly documented. The present study was designed to investigate the damaging effects of various deicing chemicals and exposure conditions on cement paste and concrete. It was anticipated that the investigation would also lead to a better understanding of damage mechanisms of deicing chemicals.

2. Experimental work

Five deicing chemicals, calcium chloride ($CaCl_2$), calcium chloride with a corrosion inhibitor ($CaCl_2$-inhib), sodium chloride (NaCl), potassium acetate (K Acetate), and an agricultural deicing product (Agr-deicing), and two exposure conditions, wetting–drying (W–D) and freezing–thawing (F–T) cycles, were considered in the present study. Physical (mass loss and scaling), mechanical (strength), chemical (ion penetration and crystalline reaction products), and micro-structural properties of the paste and concrete were evaluated. The experimental regimen is presented in Table 1.

2.1. Concrete and deicing materials

Portland cement (PC), Type I/II, was used for both paste and concrete samples. Table 2 shows the chemical composition of the cement. Air entraining agent (AEA) was used in both paste and concrete samples to obtain a designated air content of 6%. The paste had a water-to-cement ratio (w/c) of 0.4. The concrete had 2.5 cm nominal maximum aggregate size (NMSA) limestone (LS) and river sand with a fineness modulus of 2.83. Its mixture propor-

Table 1
Experimental regimen

Sample	Chemical	Exposure	No. of samples	Testing time (cycles)		
				Weight loss	Scaling	Compressive strength
Paste (5-cm cube)	Distilled water NaCl $CaCl_2$ $CaCl_2$-inhib K Acetate Agr-deicing	W–D	15 for each chemical	10, 20, 30, 40, 50, 60, 130	20, 40, 60, 130	20, 40, 60, 130
	Distilled water NaCl $CaCl_2$ $CaCl_2$-inhib K Acetate Agr-deicing	F–T	12 for each chemical	5, 10, 15, 20, 25, 30, 35, 40, 45, 50, 55, 60	20, 40, 60	20, 40, 60
Concrete (10-cm cube)	Distilled water NaCl $CaCl_2$ $CaCl_2$-inhib K Acetate Agr-deicing	W–D	12 for each chemical	10, 20, 30, 40, 50, 60	20, 40, 60	20, 40, 60
	Distilled water NaCl $CaCl_2$ $CaCl_2$-inhib K Acetate Agr-deicing	F–T	12 for each chemical	5, 10, 15, 20, 25, 30, 35, 40, 45, 50, 55, 60	20, 40, 60	20, 40, 60
				Ion penetration	XRD	SEM/EDX
Concrete (9-cm cube with ponding)	Distilled water NaCl $CaCl_2$ $CaCl_2$-inhib K Acetate Agr-deicing	W–D	3 for each chemical	20, 60	20, 60	60

Table 2
Chemical compositions of Type I/II cement

Chemical compounds	%
CaO	62.32
SiO_2	20.75
Al_2O_3	4.49
Fe_2O_3	3.45
MgO	2.88
K_2O	0.67
Na_2O	0.09
$(Na_2O)_{eq}$[a]	0.53
SO_3	2.74
TiO_2	0.34
P_2O_5	0.10
LOI	0.10
C_3S	53.09
C_2S	19.44
C_3A	6.04
C_4AF	10.50

[a] $(Na_2O)_{eq} = Na_2O + 0.658K_2O$.

tion was 0.48 (water):1.00 (PC):2.17 (sand):2.76 (LS). The high w/c (0.48) was used to achieve scaling damage of tested samples in a relative short time period.

The five deicing chemicals, $CaCl_2$, $CaCl_2$-inhib, NaCl, K Acetate, and Agr-deicing, were directly received from suppliers. NaCl and $CaCl_2$ deicing chemicals were selected because of their wide applications. $CaCl_2$-inhib deicing chemical was employed to evaluate the damaging effect of inhibitor on concrete. The corrosion inhibitor (tetraethanolamine (TEA), approximately 2000 ppm) was pre-mixed in the $CaCl_2$ solution. K Acetate is a more expensive alternative to chloride deicing chemical. It is commonly used at airfield facilities, where its lower corrosiveness makes it economical to the more damaging chlorides. The K Acetate used was a 50% (by weight) aqueous potassium acetate solution with less than 1% silicate phosphate-based corrosion inhibitor. The Agr-deicing chemical is an organic product derived from an agricultural by-product that has recently become available on the commercial market. The chemical components of the Agr-deicing product can be found in Table 3. It looks more like a gelatinous paste than a solution. The pH value of the Agr-deicing product was 7.8.

Table 3
Chemical compositions of the agricultural deicing chemical

	% By weight
Component groups	
Dissolved solids	74.84
Ash	22.81
Crude protein	19.44
Nitrogen compounds (as N)	3.11
Alpha-amino nitrogen compounds	0.41
Major compounds	
Sucrose	13.13
Raffinose	3.96
Betaine	8.95
Potassium	8.85
Sodium	1.98
Chloride	1.83
Sulfate	2.10
Pyrrolidone carboxylic acid	6.29

Table 4
Concentrations of deicing solutions employed

Chemical	Concentration (% solid, by weight)	
	For W–D exposure	For F–T exposure
NaCl	26.5	13.3
$CaCl_2$	37.9	9.5
$CaCl_2$-inhib	39.9	10.0
K Acetate	54.5	13.6
Agr-deicing	Not available	Diluted (chemical:water = 1:3)

Table 4 shows the concentrations of the deicing solutions used in the present study. The chemical concentrations for W–D exposure were directly measured from the chemicals received. Use of the different concentrations was primarily due to the consideration that users generally apply the deicing chemicals received from suppliers directly to concrete pavements. These chemical concentrations were high, and they could also maximize the potential chemical interaction between deicing chemical and paste or concrete. Diluted deicing chemical solutions were used in F–T exposures so that paste and concrete samples would freeze under the designed F–T condition.

2.2. Samples and test methods

2.2.1. General samples and exposure conditions

Fifteen paste samples and 12 concrete samples were prepared for each exposure condition (one deicing chemical under a given exposure condition). The paste samples had a size of $5 \times 5 \times 5$ cm, and the concrete samples had a size of $10 \times 10 \times 10$ cm.

After 7 days of a standard curing (ASTM C192), the samples were subjected to deicing solutions in plastic containers. For W–D exposure, samples were immersed in distilled water or a deicing solution in a container and stored in a refrigerator at 4.4 ± 1.5 °C for 15 h. Then, the samples were taken out of the container and laid on a paper towel to dry in air (approximately 23 °C and 50% RH) for 9 h. Thus, one W–D cycle took a total of 24 h.

For F–T cycling, samples were immersed in water or a deicing solution in a container and stored in a freezer at -20 ± 1.0 °C for 15 h. Then, the samples were taken out of the container to be thawed for 9 h. To facilitate thawing, the containers, together with the frozen samples and deicing solutions, were placed in a larger tub filled with warm water so that the frozen solutions were completely thawed within 4 h. The samples then remained in the water before being frozen again. One F–T cycle also took a total of 24–15 h in a frozen state and 9 h in a thawed state.

The deicing solutions in the containers were changed every 10 cycles for F–T samples, and every 20 cycles for W–D samples.

2.2.2. Mass change, scaling damage and compressive strength test methods

At every five cycles, the F–T specimens were removed and at every 10 cycles the W–D specimens were taken out of the container for mass measurement. First, the specimens were placed in a static tub of tap water and loose particles on the samples were removed gently by hand. Next, the specimens were laid on a paper towel to dry and, if the sample was not too friable, blotted with paper towels. Samples were rotated periodically to facilitate even drying of all faces. After 20–25 min of drying, samples were weighed to the nearest hundredth of a gram.

At every 20 W–D or F–T cycles, four paste and four concrete samples were removed from deicing solutions for scaling evaluations, and three paste and three concrete samples were used for compressive strength tests. Scaling damages were evaluated by the visual rating of the sample surface conditions based on Table 5. Compression tests on both paste and concrete samples were conducted according to ASTM C 109.

2.2.3. XRD and SEM samples and tests

Another set of concrete samples, two for each deicing chemical, was prepared for the ion penetration, X-ray diffraction (XRD) and scanning electron microscope (SEM) tests. Cubic plastic molds with a dimension of $9 \times 9 \times 10$ cm were used for casting 9-cm^3 samples, thus leaving a space of 1 cm at the top of each sample as a pond for the deicing solution. After the samples were cured in a standard curing room (ASTM C192) for 7 days, a marine sealant was applied to the edge of the sample surface so as to restrict chemical access from the sides. After 48 h drying of the marine sealant, deicing solutions were poured onto the sample surfaces (into the pond) to a depth of approximately 0.8 cm. The samples were then subjected to W–D cycling. For one W–D cycle, the samples (together with the deicing solution in the pond) were stored in a refrigerator (4.4 ± 1.5 °C) for 15 h. Then, the samples were taken out of the refrigerator, the deicing solutions were poured off, and the samples were dried in air (approximately 23 °C and 50% R.H.) for 9 h.

At 20 and 60 W–D cycles, seven powder samples were taken using a hand drill from seven uniform layers, with a total depth of 3.5 cm from the sample surface, of each concrete sample. The powder samples were passed through a #50 sieve and then used for ion penetration tests (IPT). Free sodium (Na) and potassium (K) ion concentrations in the samples were estimated by a soluble cation exchange method. In this method, 1 M NH_4OAc was used as an extraction solution. An atomic adsorption/emission spectrometer was used, by emission, to determine the sodium and potassium ion concentration [12]. Free chloride (Cl) concentration was measured by the saturated mercury(II) thiocyanate, $Hg(SCN)_2$, extraction method [13]. In this method, 0.01 M $Ca(NO_3)_2 \cdot 4H_2O$, together with ferric(III) nitrate nonahydrate, was used as the extraction solution. Chloride ions displace thiocyanate, in the presence of ferric iron, to form a highly colored ferric thiocyanate complex. Chloride concentration in the extract was determined by comparing with standard chloride working solutions, using a silver nitrate solution as an indicator.

Another powder sample was also taken from the surface layer (within 0.5 cm from the surface) of each concrete sample and used for XRD analysis. Siemens D500 diffractometer, with CuKα radiation, 50 kV, and 27 mA, was employed. The goniometer ran from 5° to 70° at a speed of 0.5 deg/min. The XRD patterns/spectrums were analyzed with MDI JADE 6.5 software.

SEM imaging, together with energy dispersive X-ray (EDX) analysis, was performed on the concrete samples at 60 W–D cycles. A small section, $1.20 \times 1.20 \times 0.75$ cm ($w \times l \times d$), was cut from the corner of each concrete sample and its interior surface was polished gently with a silicon carbide grinding without any lubricating solution. These polished samples were then examined under the JEOL JSM-840A SEM at a voltage of 20 kV. It was noted that precipitation and cracks might be induced during the sample preparation. The discussions in the paper (Section 3.1.6) were made under the condition that all samples were prepared with minimum polishing under the same condition.

Table 5
Visual rating of scaling damage

Rating	Description
0	No scaling
1	Slight scaling (small flakes, $\leqslant 1$ cm^2, visible on sample surface)
2	Slight to moderate scaling (large flakes visible on sample surface and sample edge damage noticeable)
3	Moderate scaling (sample edge damage and some coarse aggregate visible)
4	Moderate to severe scaling
5	Severe scaling (chunks coming out of surfaces and edges, scaling depth >0.3 cm, and coarse aggregate visible over entire surface)

3. Results and discussion

3.1. W–D cycling

3.1.1. Mass change

Fig. 1 presents the mass changes of paste and concrete samples subjected to different deicing solutions under W–D cycling. As observed in Fig. 1a, paste samples immersed in water and NaCl deicing solution experienced a slow and steady mass gain with time, while samples exposed to other chemicals displayed a different degree of mass loss. The mass gain of the paste and concrete immersed in water and other deicing chemicals has been reported by other researchers [14]. The authors considered

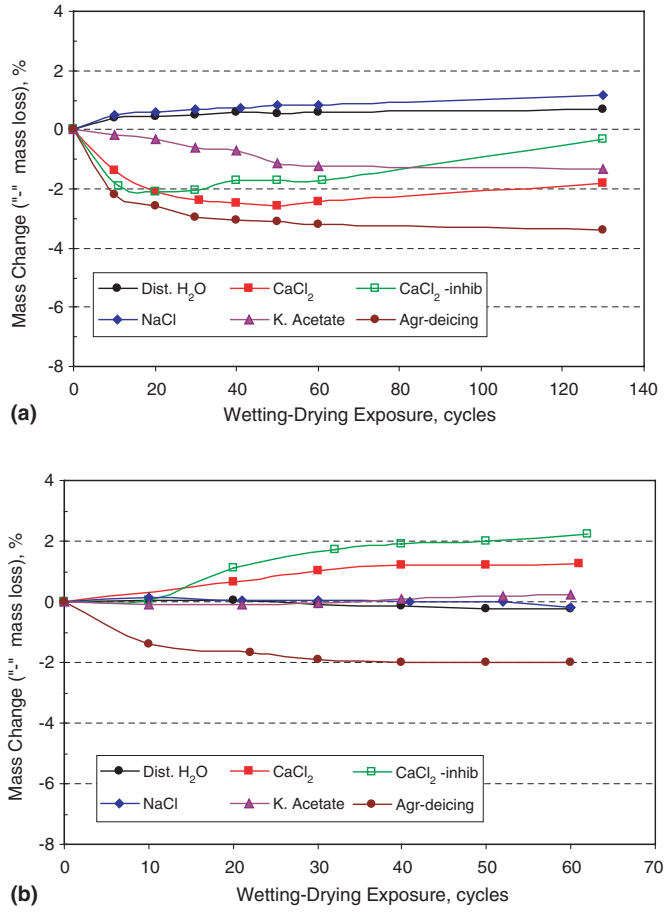

Fig. 1. Mass change of samples under W–D cycling: (a) paste and (b) concrete.

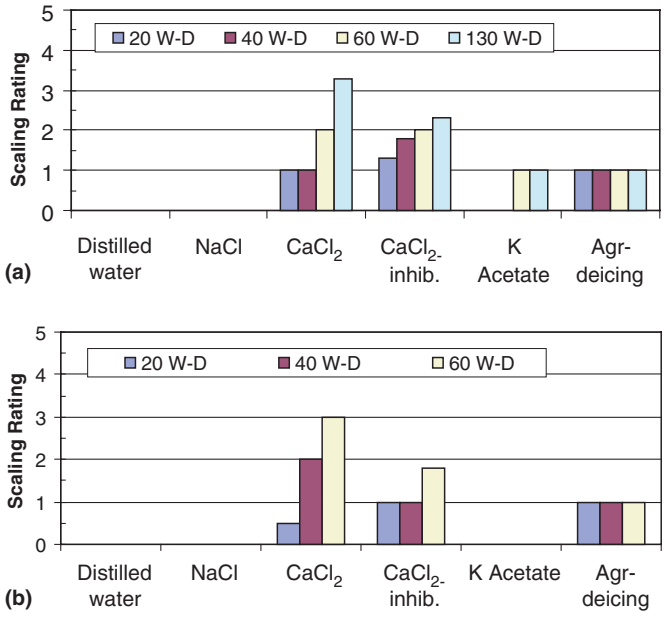

Fig. 2. Scaling rating of samples under W–D cycling: (a) paste and (b) concrete. *Notes*: The scale rating ranged from 0 to 5, with 0 for no scaling and 5 for severe scaling (Table 5); each datum in the figure represents the average value of four samples; the empty bar spaces indicate the scale rating of 0.

that such a mass gain was closely related to the cement hydration and concrete micro-structure change with time. In the present study, a short curing time (7 days) was selected to intensify deicing damage of tested samples so as to differentiate the degrees of damage from different deicing chemicals. Due to this short curing time, cement in paste and concrete would continue to hydrate when the samples were immersed in water or deicing solutions. The continuous cement hydration consumed pore fluid, leaving the samples in an unsaturated state. It also produced more C–S–H, which had a large surface area to adsorb water. The samples therefore continued to gain mass until maximum saturation was reached. This mechanism accounted for the steady mass gain observed in the samples exposed to water throughout the testing period. Mass gain of the samples exposed to deicing chemical solutions could also result from salt precipitation on sample surfaces and in pore spaces. White precipitates observed on exterior surfaces of the NaCl-immersed samples at 60 W–D cycles were responsible for partial mass gain of the sample.

In contrast to the water and NaCl-immersed samples, K Acetate-immersed samples displayed a steady mass lost at a slow rate, approximately 1.25% at 130 W–D cycles. $CaCl_2$-immersed and $CaCl_2$-inhib-immersed samples exhibited a rapid mass loss in the early W–D period (within 20 cycles). After 20 W–D cycles, the rates of mass loss in both $CaCl_2$-immersed and $CaCl_2$-inhib-immersed samples were significantly reduced. After 60 cycles, the rates of mass loss became negative although moderate scaling was observed (Fig. 2a). Due to the scaling, the volume of the samples reduced, and thus the negative rates of mass loss indicated that the samples with scaling damage actually gained mass. The authors believed that such mass changes in these samples were associated with the scaling development. Scaling damage could influence paste/concrete mass change in two different ways: (1) mass loss might occur if materials were fallen off from the body of the paste/concrete; and (2) mass gain might take place if additional free surfaces (such as cracks) generated in the paste/concrete without significant loss of concrete materials. The free surfaces would adsorb more fluid from the solution, thus increasing sample mass. It was noticed that the mass loss of the $CaCl_2$-inhib-immersed samples was more negative than that of the $CaCl_2$-immersed samples. This suggested that more free surfaces might exist in the $CaCl_2$-inhib-immersed samples.

Among all deicing chemicals tested, the Agr-deicing chemical provided its pastes with the highest initial mass loss, 2.2% in the first 10 W–D cycles. The mass loss continued until 30 W–D cycles. After 30 W–D cycles, the sample mass loss became steady. The Agr-deicing chemical contained over 32% of sweet or acid substances (sucrose, raffinose, betaine, and pyrrolidone carboxylic acid), 8.85% potassium, 1.98% sodium, 1.83% chloride and 2.01% sul-

fate (Table 3) and had a pH value of 7.8. The mass losses of the samples were presumed due to the organic and/or acid attack of the chemical on cementitious materials. As shown later, a considerable amount of micro-pores was observed on the sample surface, which corresponded to the sample mass loss.

Fig. 1b illustrates mass changes of concrete samples subjected to different deicing solutions under W–D cycling. As observed in this figure, samples immersed in water, K Acetate, and NaCl solutions exhibited very limited mass change. This implied that the mass changes in pastes were significantly decreased by addition of aggregate into the system. Aggregate could assist concrete to gain mass in two ways: (1) imbibing fluid from the solutions, and (2) resisting drying shrinkage of paste, and therefore reducing concrete cracking and scaling. As a result, unlike paste samples, both $CaCl_2$- and $CaCl_2$-inhib-immersed concrete samples gained a relatively large amount of mass under W–D cycling. Samples immersed in the $CaCl_2$-inhib solution gained more mass than the samples in the $CaCl_2$ solution. Concrete samples immersed in the Agr-deicing chemical were the only ones that lost mass significantly under W–D cycling. The mass loss reached an asymptotic maximum of about 2% mass loss at 20 W–D cycles, and it remained thereafter.

3.1.2. Scaling

Fig. 2 presents the average visual scale ratings of paste and concrete samples (four in a group) subjected to different deicing chemicals under W–D cycling. The mechanisms of concrete scaling as well as the deicing chemical effects have been briefly discussed at the beginning of the paper.

Fig. 2a illustrates that paste samples submerged in distilled water and NaCl deicing solution showed no scaling damage (scale rating = 0) throughout the entire tests (up to 130 W–D cycles). Paste samples submerged in K Acetate deicing solutions displayed minor damage (scale rating = 1.0) after 60 W–D cycles. Samples immersed in the Agr-deicing solution had a constant scaling value of 1.0 from 20 to 130 cycles due to the micro-pores observed on the sample surfaces (Fig. 3). Samples immersed in $CaCl_2$ and $CaCl_2$-inhib solutions demonstrated increasing scaling with W–D cycles.

Compared with paste samples, concrete samples (Fig. 2b) immersed in $CaCl_2$ and $CaCl_2$-inhib solutions displayed less scaling damage. This was probably because concrete generally had a small volume percentage of paste to react with deicing chemicals. However, the Agr-deicing-immersed samples exhibited a constant scale rating due to existence of micro-pores. These micro-pores were observed, as shown in Fig. 3, on the surfaces of all Agr-deicing-immersed samples (paste and concrete under W–D and F–T cycling).

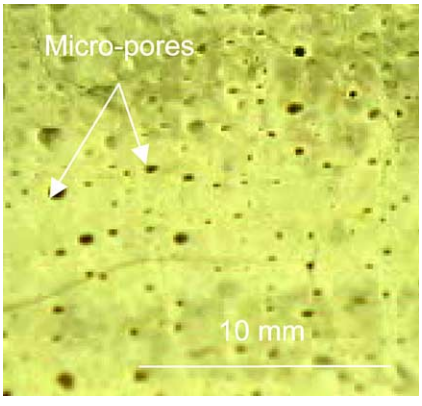

Fig. 3. Micro-pores on a Geomelt immersed sample (paste, 60 W–D cycles).

3.1.3. Strength

Fig. 4 presents compressive strength of paste and concrete samples under W–D cycling. Generally, the strength loss was associated with the scaling damage of the samples (such as that of $CaCl_2$- and $CaCl_2$-inhib-immersed samples), but some mild scaling did not always cause paste or concrete strength loss (such as K Acetate- and Agr-deicing-immersed samples).

As observed in Fig. 4a, the water-immersed paste samples increased strength with the exposure time due to continuous cement hydration. Paste samples exposed to all deicing solutions showed comparable strength to the water-immersed sample at 20 W–D cycles, but they all exhibited strength loss thereafter. The strength loss of the paste samples at 60 W–D cycles, from the highest to the lowest, was $CaCl_2$-inhib, $CaCl_2$, NaCl, Agr-deicing and K Acetate-immersed samples.

Fig. 4b illustrates that all concrete samples had much lower strength than the corresponding paste samples. This was partially due to the higher w/c used (0.48 for

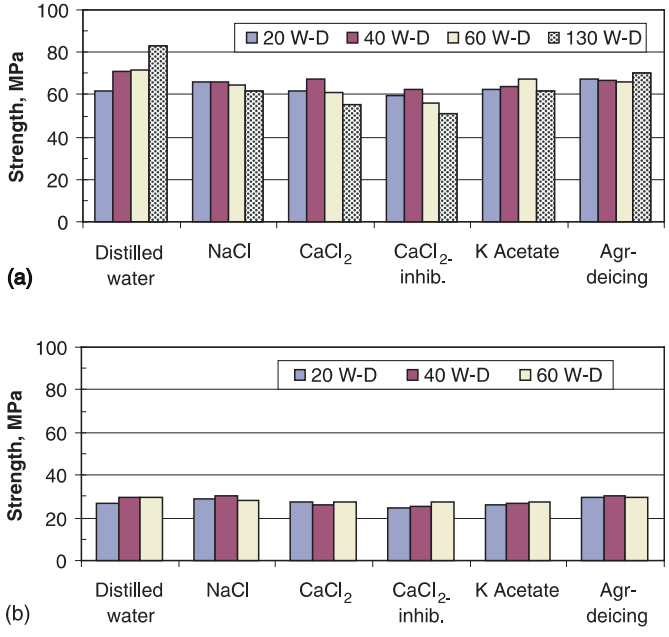

Fig. 4. Compressive strength of samples under W–D cycling: (a) paste and (b) concrete.

concrete and 0.4 for paste). However, under W–D cycling, no significant changes in concrete strength with exposure time occurred in any of the tested samples. Although having moderate scaling damage, the $CaCl_2$-immersed and $CaCl_2$-inhib-immersed samples had less than 10% strength loss when compared with the water-immersed samples. It inferred that the scaling damage only influenced the surface concrete, where cement content was high, and it had little effect on the body concrete property (such as strength). The negative effect of surface scaling might also be offset by the accelerated cement hydration in the chloride-related solutions.

3.1.4. Ion penetration

Aggressive chemical ion concentrations (such as chloride, sodium, and potassium ions) of samples exposed to distilled water and deicing chemicals under 20 and 60 W–D cycling were evaluated. The rate and depth of the chemical ion penetration were presumably related to the degree of concrete damage resulting from the reaction between the deicing chemical and concrete materials. Fig. 5 illustrates ion concentration profiles of some concrete samples under W–D cycling. Generally, for all samples immersed in deicing solutions, ion concentrations decreased with sample depth and increased with exposure time. However, ion concentrations of the water-immersed sample had a small variation with the sample depth and exposure time. The average chloride (Cl^-), sodium (Na^+), and potassium (K^+) ion concentrations within the layer 3.5 cm from the surface of the water-immersed concrete sample subjected to 60 W–D cycles were approximately 7, 580 and 490 ppm, respectively. These results were used as a reference to the samples immersed in deicing chemicals.

Fig. 5a and b shows chloride ion concentrations in two calcium chloride-related samples (without and with corrosion inhibitor). It was observed that at 20 W–D cycles, the chloride ion concentration in the $CaCl_2$-inhib-immersed sample was slightly lower than that in the $CaCl_2$-immersed sample at a given depth, especially in the near-surface layers. At 60 W–D cycles, chloride ion concentrations in both $CaCl_2$-immersed and $CaCl_2$-inhib-immersed samples appeared almost the same at a given

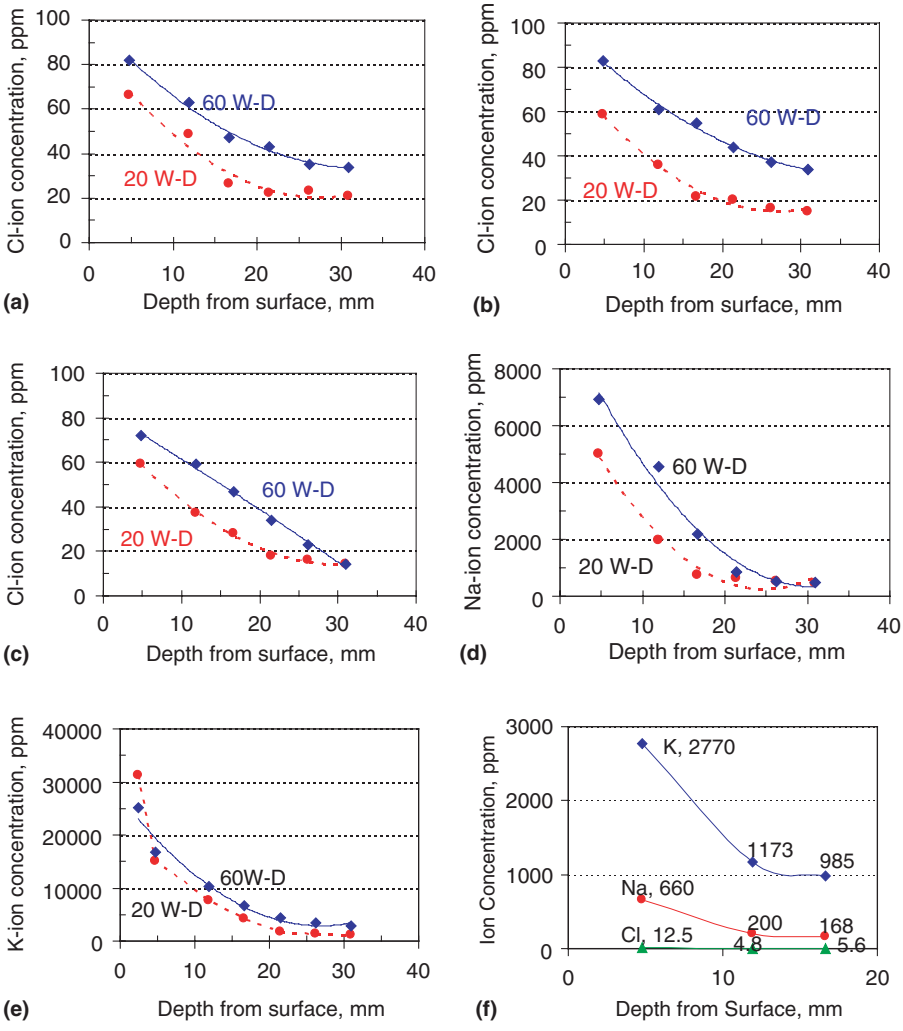

Fig. 5. Ion penetration in concrete samples: (a) chloride ions in $CaCl_2$ samples, (b) chloride ions in $CaCl_2$-inhib samples, (c) chloride ions in NaCl samples, (d) sodium ions in NaCl samples, (e) potassium ions in K Acetate samples and (f) ions in the 20 W–D Agr-deicing sample.

depth, and they were all higher than those in the samples at 20 W–D cycles. This observation indicated that the rate of the chloride penetration in the $CaCl_2$-inhib-immersed samples increased more rapidly than that in the $CaCl_2$-immersed samples with W–D cycles. At a depth greater than 2.6 cm, only a small alteration was observed in the tested samples. This result was consistent with some previous research [4]. However, at the maximum sampling depth (average 3.1 cm), chloride concentrations in the $CaCl_2$-immersed samples were still five times that in water-immersed sample at 60 W–D cycles. This implied that the chloride ions penetrated much deeper than the depth tested, and they might damage concrete or reinforcing steel at a greater depth.

Fig. 5c illustrates that at 20 W–D cycles, chloride ion concentration of the NaCl-immersed sample was similar to that of the $CaCl_2$-inhib-immersed sample (Fig. 5b). At 60 W–D cycles, chloride ion concentration of the NaCl-immersed sample was lower than that of the two $CaCl_2$-related samples, and the rate of ion penetration decreased linearly with sample depth. At a depth of 3.1 cm, the chloride concentration was 14 ppm for the NaCl-immersed sample at 60 W–D cycles, while it was 34 ppm for the $CaCl_2$-related samples. As a result, the damage due to chloride in the NaCl deicing chemical to concrete materials was limited when compared with the chloride damage caused by the $CaCl_2$ and $CaCl_2$-inhib deicing chemicals.

It was noted that sodium concentration of the NaCl-immersed sample (Fig. 5d) was also high, especially in the near-surface layer of concrete (over 5000 and 7000 ppm at 20 and 60 W–D cycles, respectively). Nevertheless, it dropped considerably with sample depth. At a depth of 2.6 cm, sodium concentrations of the samples at 20 and 60 W–D cycles were almost the same, all close to that in the water-immersed sample (580 ppm). This implied that the NaCl deicing chemical might penetrate into the concrete no more than 2.6 cm in depth. The limit penetration depth of sodium and especially chloride ions from the NaCl deicing chemical might account for the low mass loss and low scale rating of this sample (Figs. 1 and 2). Based on Berube et al. [15], the high sodium concentration in the near-surface layer of the concrete might not cause severe ASR owing to a decreased OH^- concentration in this area.

Fig. 5e exhibits potassium profiles in the samples exposed to K Acetate deicing chemical. The potassium concentrations were high in the surface layer (over 30,000 ppm); but they dropped rapidly with the distance from the concrete surface. At a depth of 3.1 cm, potassium concentrations were only 1190 ppm and 2800 ppm for the samples subjected to 20 and 60 W–D cycles, respectively. Previous research suggested that due to its small hydrated radius, potassium might produce less expansion in ASR or be less destructive to concrete than sodium [16]. Also because the high potassium concentration decreased rapidly with depth, the reaction between the K Acetate deicing chemical and paste or concrete might occur only on surface. As a result, only minor scaling damage (scale rating $\leqslant 1.0$) was observed on the K Acetate-immersed paste samples, and this scaling damage did not influence the paste or concrete strength.

Fig. 5f displays the ion concentrations in the concrete sample exposed to the Agr-deicing chemical at 60 W–D cycles. At the depth of 0.5 cm, potassium, sodium, and chloride ion concentrations of the sample were 2770, 660, and 12.5 ppm, respectively. At a depth of 1.2 cm, these ion concentrations were reduced more than half (approximately 985, 168 and 5.6 ppm for potassium, sodium, and chloride ion concentrations, respectively). At a greater depth (>1.2 cm), these ion concentrations changed very little. This implied that the Agr-deicing chemical might penetrate only a very limited distance from the concrete surface. Because of the relatively low chemical ion concentrations, together with their limited penetrations, the Agr-deicing chemical had little damaging effect on concrete integrity and strength.

3.1.5. XRD analyses

Fig. 6 displays XRD patterns of concrete samples immersed in distilled water and various deicing solutions at 60 W–D cycles. As expected, the crystalline phases of the water-immersed sample contained quartz, calcite and feldspathic minerals from the fine aggregate (Fig. 6a). Although albite and anorthite were identified, the actual mineral phases might differ slightly. Feldspathic minerals typically involved solid solution intermediate phases, e.g. like that between albite and anorthite. Hydration products, calcium hydroxide (CH) and ettringite, were also clearly identified. This XRD pattern (Fig. 6a) was used as a reference for identifying possible leaching and new crystalline reaction products in the concrete exposed to deicing chemicals.

Fig. 6b exhibits the XRD pattern of $CaCl_2$-immersed concrete sample, which was similar to that of $CaCl_2$-inhib-immersed sample. CH and ettringite peaks were hardly seen in this sample (subjected to 60 W–D cycles), neither in the sample subjected to 20 W–D cycles, which might correspond to leaching as identified in previous studies [4,6,17]. Two new peaks were observed at 8.375 Å (10.554°) and at 3.85 Å (23.082°) in the sample subjected to 60 W–D cycles. These peaks were found to match the two most intense peaks for a calcium aluminum chloride sulfate hydrate (Ca–Al–Cl–S hydrate) mineral: $Ca_8Al_4O_{12}Cl_2SO_4 \cdot 24H_2O$. The peaks were not found in the 20 W–D samples, suggesting that the mineral alteration and chemical reactions between $CaCl_2$ deicing solution and concrete constituents needed sufficient time to take place. It was noted that the relative intensity of Ca–Al–Cl–S hydrate (compared with intensity of quartz) of the $CaCl_2$-inhib-immersed sample appeared higher than that of the $CaCl_2$-immersed sample, indicating that more Ca–Al–Cl–S hydrate might form in the $CaCl_2$-inhib-immersed sample. The leaching of CH and ettringite in the concrete and the reaction between the deicing chemical and concrete

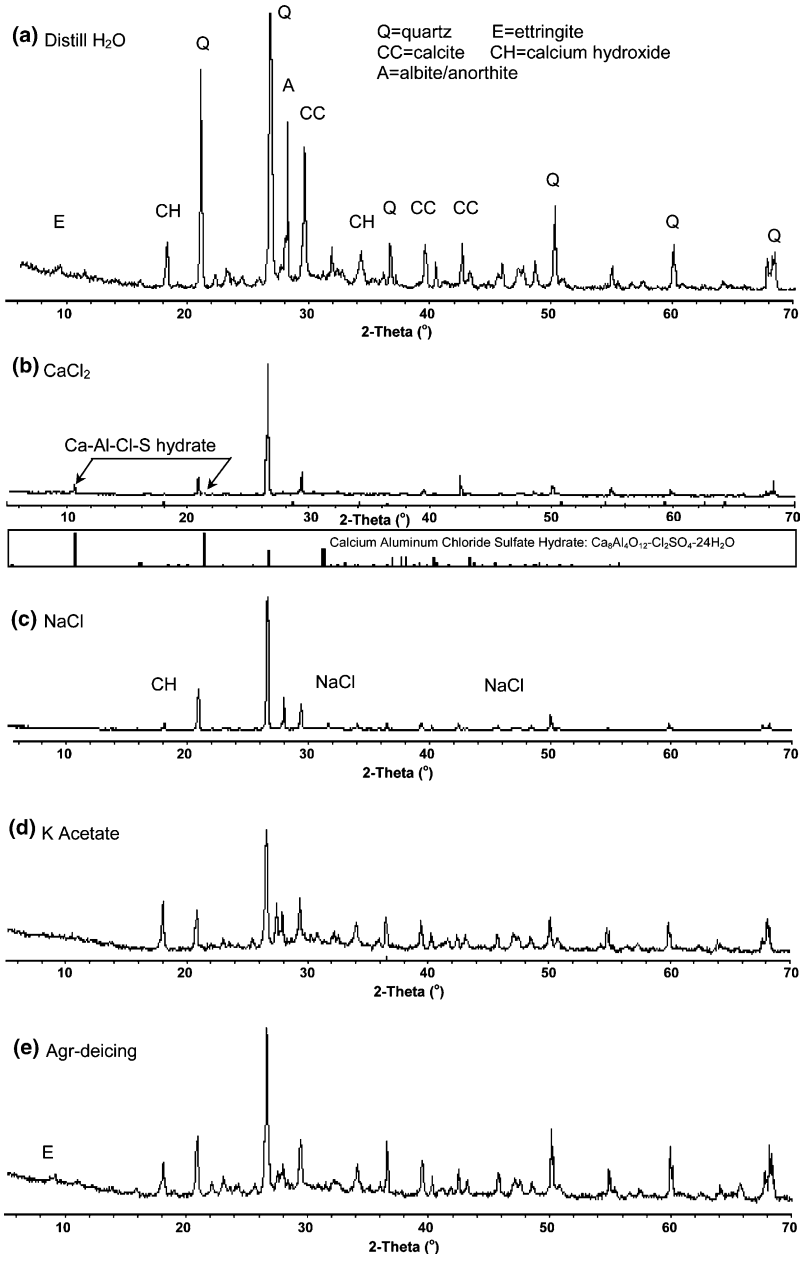

Fig. 6. XRD pattern of concrete samples under 60 W–D cycling.

materials certainly accounted for the high scale ratings of the samples (Fig. 2).

Fig. 6c illustrates the XRD pattern of concrete exposed to NaCl deicing chemicals. CH peaks were identified in this sample, but its relative intensity to quartz peak intensity was very small when compared with that in the water-immersed sample. This might be due to the relatively slow chloride penetration of this deicing chemical, which reduced the severity of the chloride attack on cement hydration products. As a result, no significant scaling was observed in the NaCl-immersed sample under W–D cycling (Fig. 2). Although previous research has suggested that concrete subjected to all chloride solutions produced chloroaluminate [18], there was no new XRD peak identified in the NaCl-immersed sample. Small halite (NaCl) peaks were detected, associated with the small amount of precipitations observed in some voids of the sample.

Fig. 6d and e presents the XRD patterns of the K Acetate-immersed sample and the Agr-deicing-immersed sample, respectively. In contrast to the samples immersed in the chloride-related deicing chemicals, the K Acetate-immersed sample displayed clear CH peaks. Ettringite peaks were not detected, probably due to alkali carbonation [19] (Section 3.1.6). No new peaks were detected in the two non-chloride samples.

Although the micro-pores observed on the sample surfaces, the Agr-deicing-immersed sample displayed both ettringite and CH peaks clearly. The XRD result inferred

that the micro-pores might result from the organic attack of the Agr-deicing chemical on concrete surface, rather than leaching of the cement and hydration materials in the acid solution. Since the Agr-deicing chemical did not penetrate very deep, this micro-pore damage might occur only up to a certainly depth; thus not impairing the paste and concrete integrity. Thus, the Agr-deicing-immersed samples demonstrated little scaling and strength loss (Figs. 2 and 4). Further research is needed to study the causes of the micro-pores.

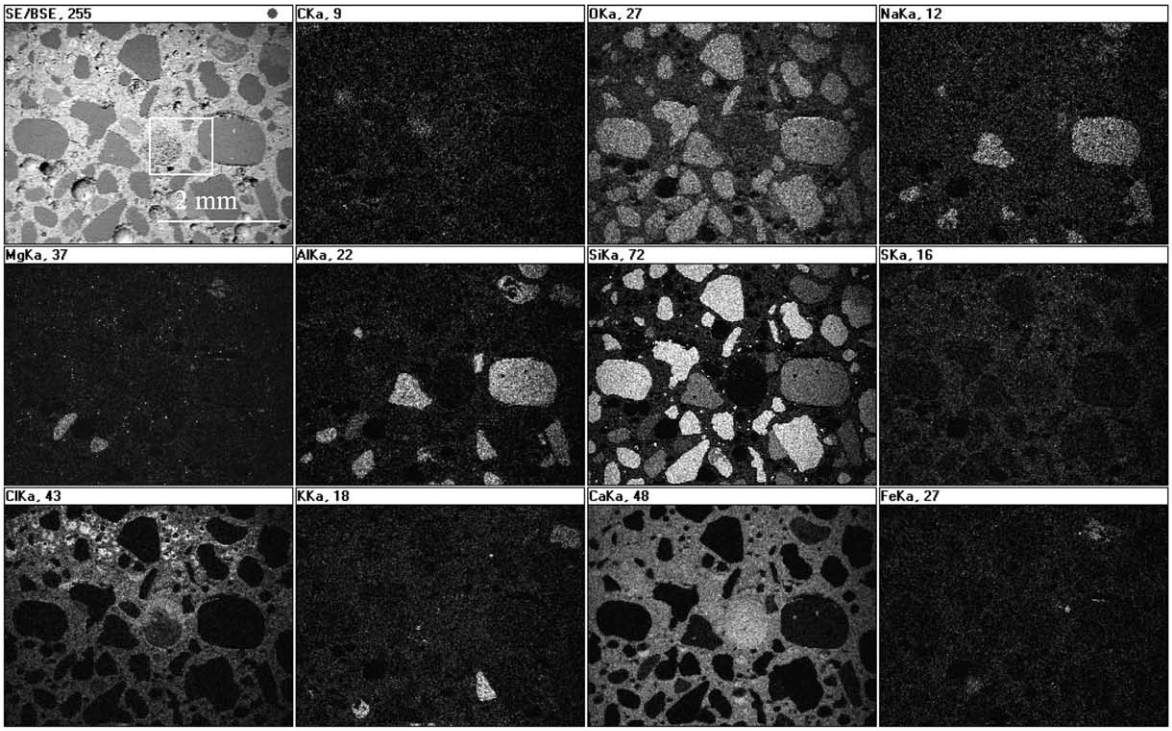

Fig. 7. Element map of concrete exposed to $CaCl_2$ deicing chemical. Element mapping at (a) 25× and (b) 100×.

3.1.6. SEM image and EDX analyses

All SEM images were taken from the polished surface that was approximately 7.5 mm from the exposed surface. The exposed surface is the concrete surface that was in contact with the deicing chemicals. Some EDX point analyses were done on the sides of the SEM samples at the different depths from the exposure surface. Locations of these EDX point analyses are indicated in the corresponding EDX figures.

Fig. 7 illustrates the backscatter images and element maps of the concrete sample exposed to $CaCl_2$ deicing chemical. Fig. 7a illustrates that the sample was severely cracked, and the cracks went along or radiated from aggregate and void interfaces. In the top layer of the concrete, most air voids were completely or nearly filled with precipitates. The high chloride concentration was seen in the concrete voids, cracks and paste–aggregate interfaces, generally together with precipitates. It suggested that great pressures had developed in the sample due to crystallization and precipitation. This salt crystallization and precipitation might aggravate the scaling damage and strength loss of the samples originating from leaching of CH and ettringite in the solution and the chemical reaction between the deicing chemical and concrete materials.

Fig. 7b demonstrates detailed chloride ion distribution in and near an air void in the highlighted area of Fig. 7a. The rims of high oxygen, aluminum, silica, chloride and calcium concentrations were noted on the edge of the aggregate particle. EDX point analysis (Fig. 8a) of the void indicated that the chemical substance, associated with the high chloride concentration, was only calcium, and little sulfate and magnesium were detected in this area. This signified that the high chloride concentration in the void mostly resulted from $CaCl_2$ salt precipitation, formation of calcium chloride hydrate ($3CaO \cdot CaCl_2 \cdot 12H_2O$; or $CaO \cdot CaCl_2 \cdot 2H_2O$), and/or adsorption of chloride ions by C–S–H [20]. However, other point analyses were conducted at different depths of the same sample, and the results suggested that the substance having a high chloride concentration was also associated with alumina and sulfate (Fig. 8b). Such a substance was possibly associated with the Ca–Al–Cl–S hydrate as detected by XRD tests. The $CaCl_2$-inhib-immersed sample showed similar cracking patterns and the EDX spectrum to the $CaCl_2$-immersed sample at 60 W–D cycles.

Fig. 9 presents the SEM image and EDX analysis of concrete exposed to NaCl deicing chemical. In this sample (Fig. 9a), most air voids looked clean. Some cracks were observed within a small region of congested air voids; but there was no crack network in the sample. The cracks did not appear to contain any precipitates. The element map showed high concentrations of both sodium and chloride ions surrounding pore edges and aggregate–paste interfaces, indicating that NaCl penetrated into these areas as identified from XRD analysis (Fig. 6c). Although no Ca–Al–Cl–S hydrate was detected in XRD test, the relative heights of calcium, chloride, sulfate and aluminum peaks in the EDX spectrum of the NaCl immersed sample

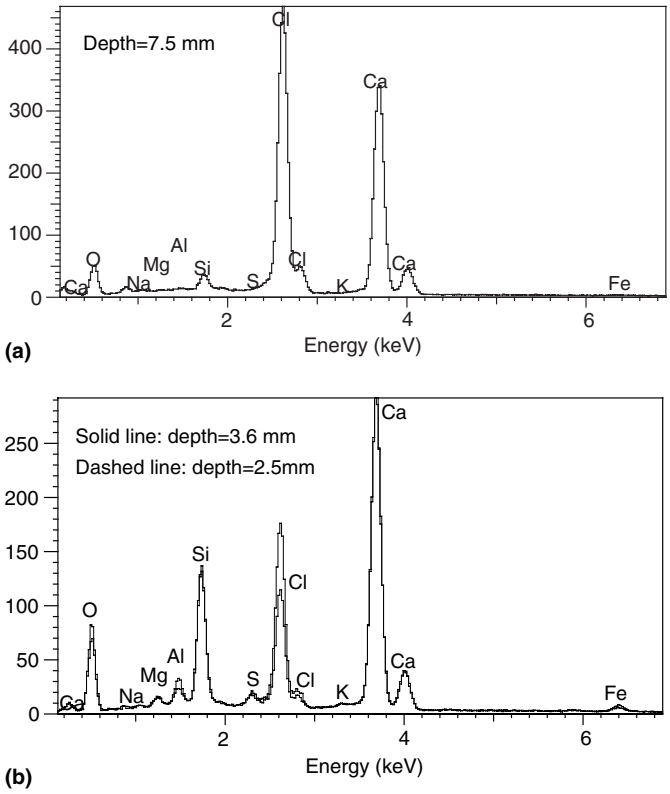

Fig. 8. Point analysis of concrete exposed to $CaCl_2$ deicing chemical. (a) Point analysis of the void in Fig. 7(b). (b) Point analysis at different depth of the sample.

(Fig. 9b) appeared similar to those of the $CaCl_2$-immersed samples. This implied that some Ca–Al–Cl–S-related phases might also be produced in the NaCl-immersed concrete. Previous researchers also suggested that concrete subjected to all chloride solutions might produce chloroaluminate, resulting from the replacement of pre-existing ettringite (chloride ions substituted for sulfate ions in the ettringite structure) [20]. This chemical reaction might be attributed to the disappearance of ettringite evidenced by the XRD analysis of the NaCl-immersed sample (Fig. 6c). Other researchers found that badly crystallized small crystals of chloroaluminate were in the cement paste, while well-formed crystals were present in air voids [15].

SEM imaging and element mapping were also performed for concrete samples immersed in K Acetate and the Agr-deicing chemicals. The two non-chloride samples exhibited little signs of significant deterioration: little cracking, no reaction rim and no significant precipitate in voids. As illustrated in Fig. 10, the sample immersed in K Acetate deicing chemical had not only a high potassium concentration but also high carbon concentrations, which signified a possible alkali carbonation of the sample [7]. The carbonation reaction would involve:

$$K^+ \text{ (from K Acetate)} + OH^- \text{ (from solution)} \rightarrow KOH;$$

and

$$2KOH + CO_2 = K_2CO_3 + H_2O$$

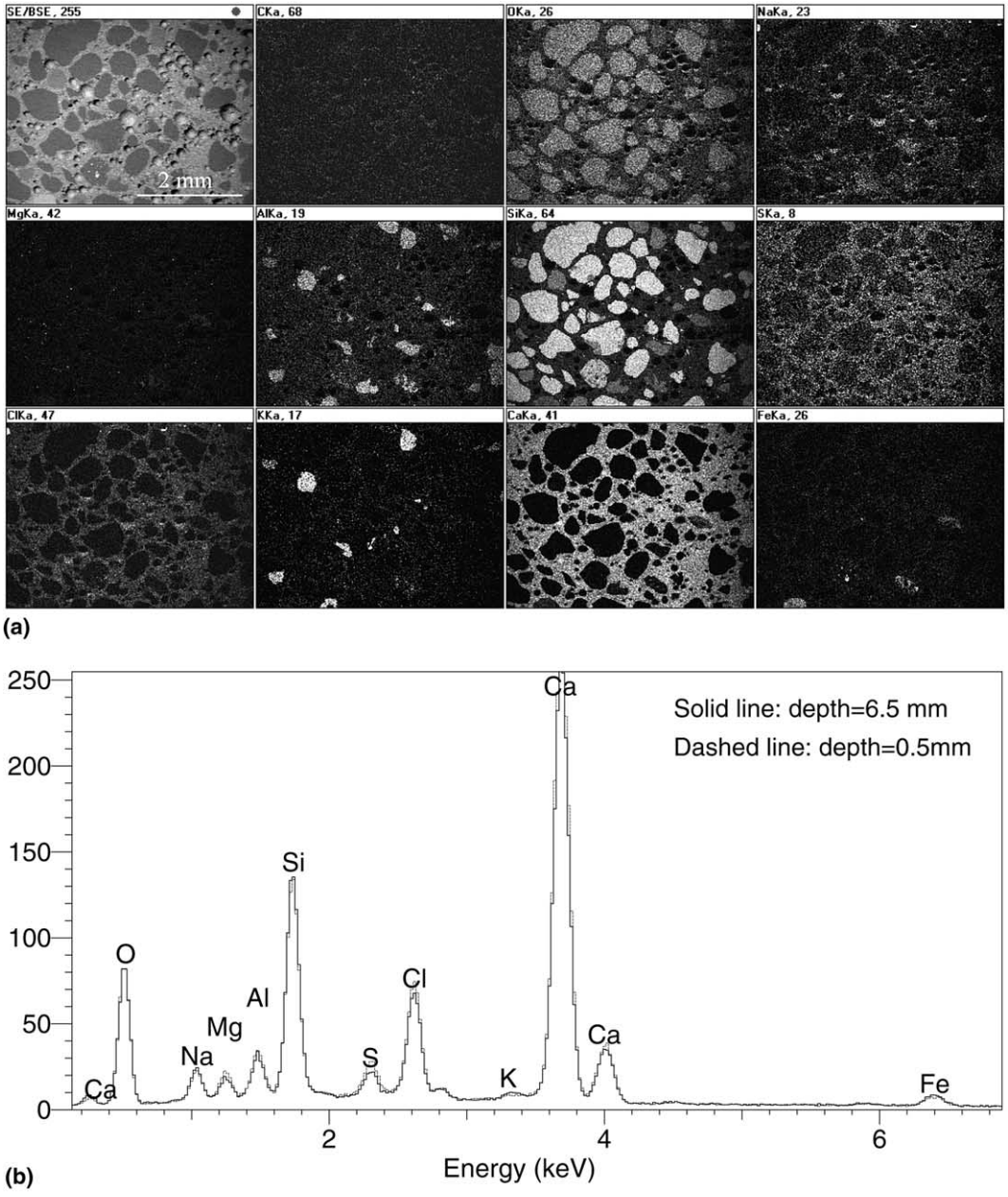

Fig. 9. EDAX analysis of concrete exposed to NaCl deicing chemical. (a) Elemental map at 25×. (b) Point analysis at different depth.

In addition to the removal of ettringite, the alkali carbonation reaction product, potassium carbonate (K_2CO_3), in the sample might further react with CH and/or anhydrate ($CaSO_4$) in the cement system. Small scale rating observed from the cement pastes exposed to the K Acetate deicing chemical might correspond to these chemical reactions (Fig. 2a).

3.2. F–T cycling

3.2.1. Mass change

Fig. 11 presents the mass changes of paste and concrete samples subjected to deicing solutions under F–T cycling. Note that not all F–T samples behaved as same as the W–D samples. Particularly, the two chloride-related samples performed very differently from others.

Similar to those under W–D cycling, paste samples (Fig. 11a) immersed in water and NaCl solution gained a minimal amount of mass under F–T cycling (0.5% for water-immersed samples and 1.0% for NaCl-immersed samples, respectively, at 60 cycles). In contrast to those under W–D cycling, K Acetate-submerged samples gained, rather than lost, a very small amount of mass under F–T cycling (0.25% at 60 cycles). It was observed that the samples underwent a minor degree of scaling at 60 F–T cycles; therefore, some mass reduction via physical loss should occur. However, this mass loss might be offset by imbibed water and possible salt crystallization, thus increasing overall mass of the samples.

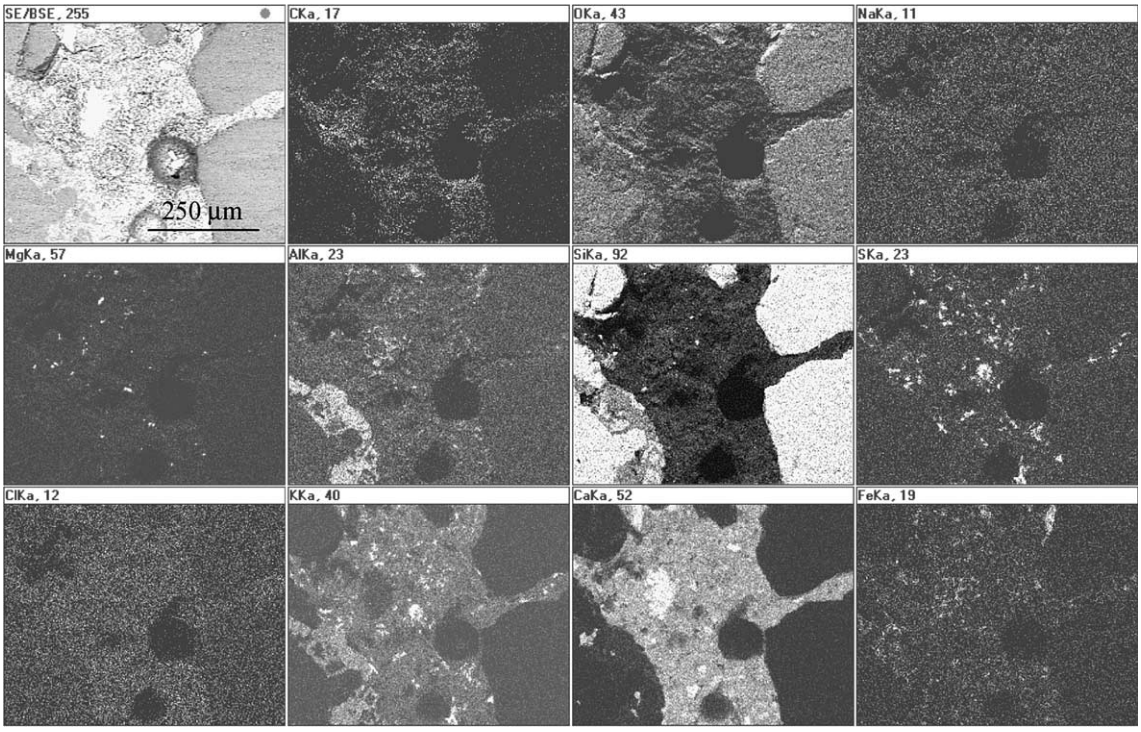

Fig. 10. Elemental map of concrete exposed to K Acetate deicing chemical (200×).

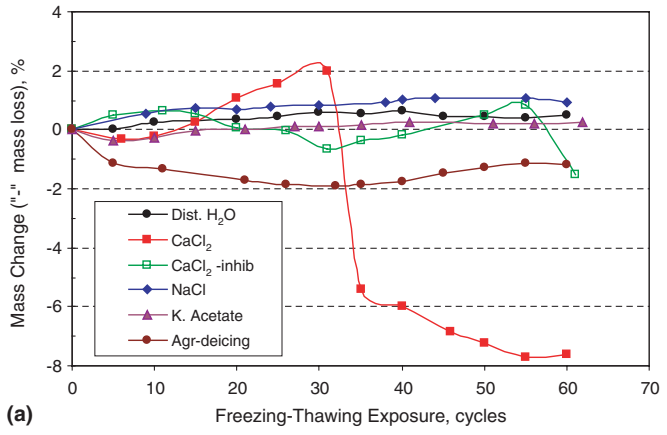

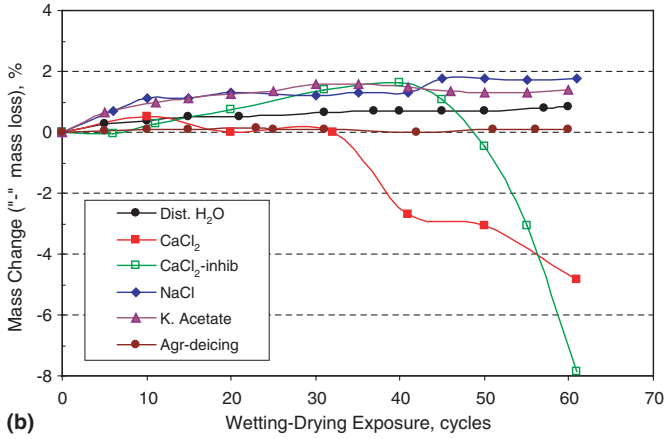

Fig. 11. Mass change of samples under F–T cycling: (a) paste and (b) concrete.

Paste samples exposed to $CaCl_2$ without corrosion inhibitor gained mass during 0–30 F–T cycles although cracking and scaling were observed at less than 10 F–T cycles. This might be again attributed to crystal precipitation and fluid absorption in the cracks. The cracks provided the samples with more free surface area, which held a large amount of moisture and salinity fluid, thus increasing the sample mass. During 30–40 F–T cycles, however, drastic mass loss occurred. The high salinity fluid on the free surfaces might osmotically draw moisture to the sample from the solution. The increased moisture content and degree of saturation of the samples made the samples more vulnerable to hydraulic, thermodynamic and osmotic pressures upon freezing. As observed, the sample surface planes were steadily swollen and then fractured as the sample mass increased during 20–30 F–T cycles. At 30 cycles, these surface layers finally sloughed off, resulting in the significant mass loss. At 60 F–T cycles, the total mass loss of the samples exceeded 7.5%.

Paste samples submerged in the $CaCl_2$-inhib deicing solution displayed a small amount (<1%) of alternative mass gain and loss during 0–55 F–T cycles. Initially, the samples gained a little mass within the first 10 cycles, and then lost a little mass through 30 cycles. Mass gain ensued during 30–55 cycles and was then followed by a sharp mass loss. Finally, mass loss of the samples totaled 1.5% at 60 F–T cycles. There was a tendency that the rapid mass loss would continue if the F–T cycles were extended. It suggested that the corrosion inhibitor only delayed crystal precipitation, thus delaying the onset of damage to samples. However, it did not reduce the ultimate damage. At

60 F–T cycles, samples immersed in the $CaCl_2$-inhib solution were about to undergo significant mass loss similar to that observed from the samples without inhibitor. Concrete test results discussed below confirmed this inference.

The paste samples immersed in the Agr-deicing solution experienced the most but steady mass loss among all samples tested under F–T cycling. The final mass loss at 60 F–T cycles was 2%, less than that observed in W–D cycling (>3%). This suggested that the rate of organic attack of the sample was reduced at a low F–T temperature condition.

Fig. 11b demonstrates the mass changes of concrete samples under F–T cycling. Before 30 F–T cycles, all samples displayed a small amount of mass gain. After 30 F–T cycles, significant mass losses were observed in both $CaCl_2$- and $CaCl_2$-inhib-immersed samples, while continuous mass gain occurred in the samples immersed in water, NaCl, K Acetate, and the Agr-deicing chemical.

Mass loss in $CaCl_2$-immersed samples began right after 30 cycles. Coincidentally, this was the same age at which the $CaCl_2$-immersed paste F–T samples began to disintegrate. Therefore, the rapid increase in mass loss of the sample might be associated with paste disintegration. Samples immersed in the $CaCl_2$-inhib solution experienced precipitous mass loss, as considerable amounts of surface material scaled off, after 40 cycles. The final mass losses were about 5% for the $CaCl_2$-immersed samples and nearly 8% for the $CaCl_2$-inhib-immersed samples at 60 F–T cycles. These concrete sample results once again implied that $CaCl_2$ with corrosion inhibitor deicing chemical could only postpone, not eliminate, concrete damage. Once mass loss began, the rate in $CaCl_2$-inhib-immersed samples was significantly greater than the rate of mass loss in $CaCl_2$-immersed samples.

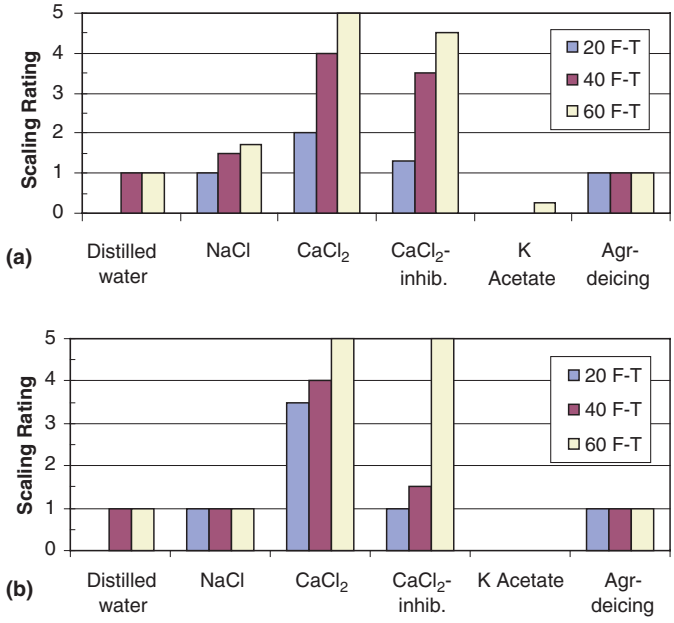

Fig. 12. Scaling rating of samples under F–T cycling: (a) paste and (b) concrete. *Notes*: The scale rating ranged from 0 to 5, with 0 for no scaling and 5 for severe scaling (Table 5); each datum in the figure represents the average value of four samples; the empty bar spaces indicate the scale rating of 0.

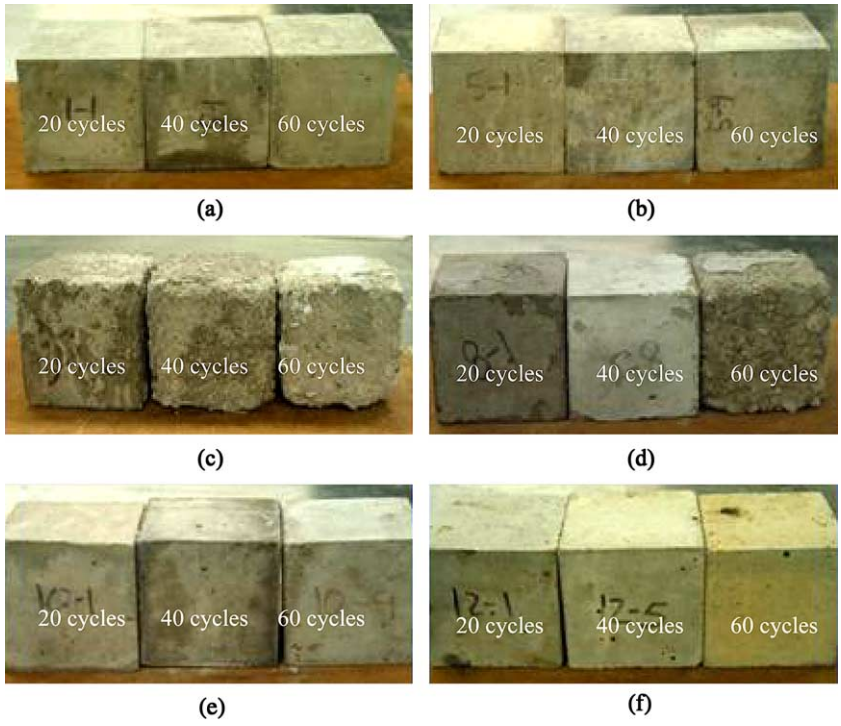

Fig. 13. Conditions of concrete samples ($5 \times 5 \times 5$ cm) exposed to deicing chemicals under F–T cycling. (a) H_2O, (b) NaCl, (c) $CaCl_2$ without inhibitor, (d) $CaCl_2$ with inhibitor, (e) K Acetate and (f) Agr-deicing.

3.2.2. Scaling

As shown in Fig. 12, damages of all samples (paste and concrete) were aggravated under F–T cycling, except for the samples immersed in the Agr-deicing solution. Similar to the trend found under W–D cycling, the samples immersed in $CaCl_2$ and $CaCl_2$-inhib solutions had more severe damage than the samples immersed in other deicing chemicals. Fig. 13 demonstrates the conditions of the concrete samples after immersed in deicing chemicals and different F–T cycles. Of these two sets of $CaCl_2$-related samples, the samples without inhibitor showed the more severe deterioration at earlier exposure (20 F–T cycles, Fig. 13c), while the samples with inhibitor displayed more severe deterioration at later exposure (60 cycles, Fig. 13d). As discussed before, the severity of damage might correspond to the rate and depth of chemical ion penetration into the concrete.

3.2.3. Strength

Fig. 14 presents compressive strength of paste and concrete samples under F–T cycling. The water-immersed paste samples under F–T cycling (Fig. 14a) gained a smaller amount of strength with exposure time than the samples under W–D cycling. This might result from the combined effect of frost damage and slow cement hydration at the low temperature. Paste samples immersed in $CaCl_2$ and $CaCl_2$-inhib solutions displayed considerable strength loss, while the samples exposed to NaCl, K Acetate, and the Agr-deicing solutions had little strength loss with increasing F–T cycles.

The concrete samples (Fig. 14b) in both $CaCl_2$ and $CaCl_2$-inhib solutions experienced dramatic strength loss (over 50%) when compared to samples immersed in water.

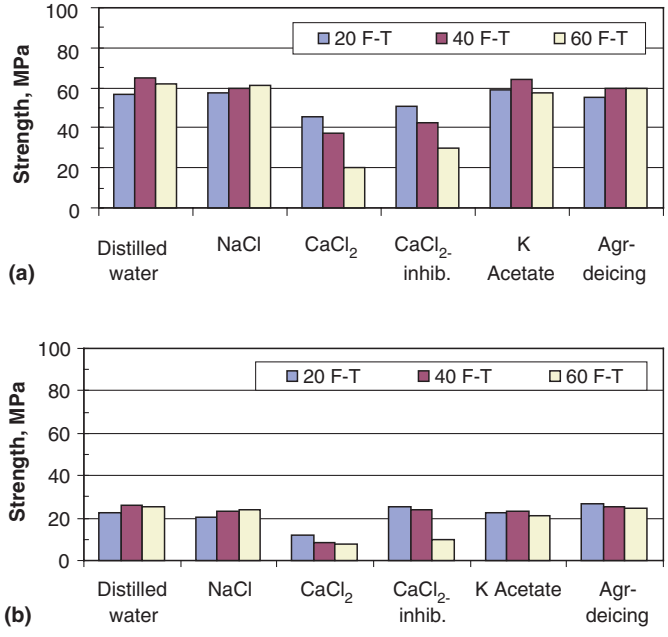

Fig. 14. Compressive strength of samples under F–T cycling: (a) paste and (b) concrete.

The $CaCl_2$-immersed concrete samples lost strength much earlier than the $CaCl_2$-inhib-immersed samples. At 20 cycles, concrete strength was 11.8 MPa for $CaCl_2$-immersed samples and 25.7 MPa for $CaCl_2$-inhib-immersed samples. At 40 F–T cycles, it was 8.5 MPa for $CaCl_2$-immersed samples and 24.0 MPa for $CaCl_2$-inhib-immersed samples. By 60 F–T cycles, strength of the $CaCl_2$-immersed samples declined steadily to 7.7 MPa, while strength of the $CaCl_2$-inhib-immersed samples dropped significantly to 9.7 MPa. The precipitous strength loss corresponded to the significant scaling (scale rating = 5.0 at 60 F–T cycles) and mass loss of the samples. Again, the corrosion inhibitor appeared to delay concrete damage, but it did not diminish damage once it began. The NaCl-immersed and Agr-deicing-immersed concrete samples had little change in strength and the K Acetate-immersed concrete samples had about 15% strength loss through 60 F–T cycles.

It was presumed that the chemical interactions between the deicing chemicals and concrete materials under F–T cycling were similar to those under W–D cycling. Therefore, no ion penetration test, XRD analysis, and SEM study were performed for the F–T samples.

4. Conclusions

The following conclusions can be drawn from the present investigation:

(1) Among the five deicing chemicals studied, two $CaCl_2$ solutions, with and without corrosion inhibitor, displayed the most severe damages to concrete materials under both W–D and F–T conditions. These severe damages, shown by the mass and strength loss of the samples, were associated with the salt crystallization and precipitation, leaching of cement hydration products (CH and ettringite), and chemical reaction between the deicing chemicals and concrete materials (Ca–Al–Cl–S hydrate formation).

(2) For the given types and concentrations of the deicing chemicals used, aggressive chemical ions penetrated at different rates into a given paste and concrete, resulting in different degrees of damage. Chloride ions from the two chloride-related deicing chemicals penetrated faster and deeper than those from the NaCl deicing chemical used. This corresponded to the severe damages in the $CaCl_2$- and $CaCl_2$-inhib-immersed samples. Chloride ions from the $CaCl_2$-inhib deicing chemical penetrated slowly at the early W–D cycling but became fast at the later W–D cycling. Addition of a corrosion inhibitor into a $CaCl_2$ deicing solution delayed the initial damage, but did not reduce the ultimate damage, to paste and concrete.

(3) The samples immersed in two non-chloride deicing chemicals, K Acetate and the agricultural deicing product, exhibited limited signs of significant

deterioration: very few small and isolated cracks, no measurable chemical reaction, and no significant precipitation in voids. These samples remained good integrity and strength throughout the tests although minor scaling was found in some K Acetate-immersed samples and significant mass loss and micro-pores were observed from the Agr-deicing-immersed samples.

(4) Under W–D cycling, measurable damages of deicing chemicals to paste and concrete were identified. Under F–T cycling, the mass change, scaling damage, and strength loss of paste and concrete samples were aggravated. The trends of the paste test results were similar to those of the concrete test results.

Acknowledgments

The present study is part of the Iowa Highway Research Board (IHRB) project (No. TR-471). The authors would like to acknowledge IHRB, Iowa Department of Transportation (Iowa DOT) and the Center for Portland Cement Concrete Pavement Technology (PCC Center) for co-sponsorship of this research. Assistance from the Material Analysis and Research Laboratory (MARL), Iowa State University, with XRD and SEM analyses is also greatly appreciated.

References

[1] Litvan GG. Frost action in cement in the presence of deicers. Cem Concr Res 1976;6(3):351–6.
[2] Setzer MJ. Action of frost and deicing chemicals. Basic phenomena and testing. In: Marchand J, Pigeon M, Zetzer M, editors. Freeze–thaw durability of concrete. London: E&FN Spon; 1997. p. 3–21.
[3] Harnick AB, Meier V, Rosli A. Combined influence of freezing and deicing salt on concrete: physical aspects. In: Sereda PJ, Litvan GG, editors. Durability of building materials and components. ASTM STP 691, 1980. p. 474–84.
[4] Hoffmann DW. Changes in structure and chemistry of cement mortars stressed by a sodium chloride solution. Cem Concr Res 1984;14(1):49–56.
[5] Kurdowski W, Duszak S, Trybalska B. Corrosion of tobermorite in strong chloride solution. In: Scrivener KL, Young JF, editors. Mechanisms of chemical degradation of cement-based systems. London: E&FN Spon; 1997. p. 114–21.
[6] Heukamp FH, Ulm FJ, Germaine JT. Mechanical properties of calcium-leached cement pastes: triaxial stress states and the influence of the pore pressures. Cem Concr Res 2001;31(5):767–74.
[7] Brown PW, Doerr A. Chemical changes in concrete due to ingress of aggressive species. Cem Concr Res 2000;30(3):411–8.
[8] Nixon PJ, Page CL, Canham I, Bollinghaus R. Influence of sodium chloride on the ASR. Adv Cem Res 1988;1:99–105.
[9] Kawamura M, Takeuchi K, Sugiyama A. Mechanisms of expansion of mortars containing reactive aggregates in NaCl solution. Cem Concr Res 1994;14:621–32.
[10] Jang J, Hagen MG, Engstrom GM, Iwasaki I. Cl^-, SO_4^{2-}, and PO_4^{3-} distribution in concrete slabs ponded by corrosion–inhibitor-added deicing salts. Adv Cem-Based Mater 1998;8(3–4):101–7.
[11] Mehta PK, Gerwick BC. Cracking–corrosion interaction in concrete exposed to marine environment. Concr Int 1982;4(10):45–51.
[12] Warncke D, Brown JR. Recommended chemical soil test procedures for the North Central Region. In: Dahnke WC, editor. North Central Region Publication 221. Fargo, ND: North Dakota Agriculture Experimental Station; 1980. p. 31–3.
[13] Gelderman RH, Denning JL, Goos RJ. Recommended chemical soil test procedures for the North Central Region. In: Dahnke WC, editor. North Central Region Publication 221. Fargo, ND: North Dakota Agriculture Experimental Station; 1980. p. 49–52.
[14] Santagata CC, Collepardi M. The effect of CMA deicers on concrete properties. Cem Concr Res 2000;30(9):1389–94.
[15] Berube MA, Dorion JF, Duchesne J, Fournier B, Vezina D. Laboratory and field investigations of the influence of sodium chloride on alkali–silica reactivity. Cem Concr Res 2003;33(1):77–84.
[16] Turanli L, Wenk HR, Monteiro PJM, Sposito G, Shomglin K. The effects of potassium and rubidium hydroxide on the alkali–silica reaction. Cem Concr Res 2003;33(11):1825–30.
[17] Chatterji S. Mechanism of $CaCl_2$ attack on portland cement concrete. Cem Concr Res 1978;8(4):461–8.
[18] Lee H, Cody RD, Cody AM, Spry PG. Effects of various deicing chemicals on pavement and concrete deterioration. In: Proceedings, mid-continent transportation symposium, Center for Transportation Research and Education, 2000. p. 151–5.
[19] Gaze ME, Crammond NJ. The formation of thaumasite in a cement:lime:sand mortar exposed to cold magnesium and potassium sulfate solutions. Cem Concr Compos 2000;22(3):209–22.
[20] Lee H, Cody RD, Cody AM, Spry PG. Effects of various deicing chemicals on pavement and concrete deterioration. In: Proceedings, mid-continent transportation symposium, Center for Transportation Research and Education, 2000. p. 151–5.